Applied Surface Science

Transport properties of water molecules confined between hydroxyapaptite surfaces: A Molecular dynamics simulation approach

Muthuramalingam Prakash [a,b], Thibault Lemaire [a,*], Devis Di Tommaso [c], Nora de Leeuw [d], Marius Lewerenz [e], Matthieu Caruel [a], Salah Naili [a]

[a] Université Paris Est, Laboratoire de Modélisation et Simulation Multi-Echelle, UMR 8208, CNRS, 94010 Créteil, France [b] SRM Research Institute and Department of Chemistry, SRM University, Kattankulathur, 603203, Tamil Nadu, India
[c] School of Biological and Chemical Sciences, Queen Mary University of London, Mile End Road, E1 4NS London, UK [d] School of Chemistry, Cardiff University, Main Building, Park Place, Cardiff, CF10 3AT, UK
[e] Université Paris Est, Laboratoire de Modélisation et Simulation Multi-Echelle, UMR 8208, CNRS, 77454, Marne la Vallée Cedex 2, France

article info

Keywords:
Molecular dynamics simulation
HAP-Water systems
Water self diffusion
H-bonding and hydroxyl dissociation

abstract

Water diffusion in the vicinity of hydroxyapatite (HAP) crystals is a key issue to describe biomineralization process. In this study, a configuration of parallel HAP platelets mimicking bone nanopores is proposed to characterize the nanoscopic transport properties of water molecules at HAP-water surface and interfaces using various potential models such as combination of the Core-Shell (CS) model, Lennard-Jones (LJ) potentials with SPC or SPC/E water models. When comparing all these potentials models, it appears that the core-shell potential for HAP together with the SPC/E water model more accurately predicts the diffusion properties of water near HAP surface. Moreover, we have been able to put into relief the possibility of observing hydroxyl (OH^-) ion dissociation that modifies the water structure near the HAP surface.

1. Introduction

Investigation of bone-material is very important to understand the physical properties at bone-material interface [1–5]. Bone min-eral phase is made of hydroxyapatite (HAP) [6] which is also present in the teeth enamel. It is often necessary to understand the phe-nomena occurring at the nanometric scale of the HAP minerals of bone (molecular unit formula [$Ca_{10}(PO_4)_6(OH)_2$]) to understand the macroscopic behaviour of this organ [7–9]. During biomin-eralization, bone-water interface plays an important role in the mechanism of bone reorganization [10]. Thus, the investigation of HAP-water interface materials received widespread attention to understand the chemical, physical and mechanical properties of these materials considering the confinement effect of water near the HAP surface [5,11–13].

Similarly, HAP scaffolds are often used in bone repair [14] and is thus the prototype model for the biomaterial adsorption stud-ies [15,16]. The metabolism of bone tissue is characterized by the surface interactions between HAP crystals, cells, water molecules and bridging proteins [17]. Numerous studies have thus been devoted to understand the interaction between HAP surfaces with biomolecules, water, ions, and gases using experimental and theo-retical methods [18–25].

In particular, it was shown that the interactions between a sur-face and water molecules may affect the local environment of the interface, modifying the diffusion properties of water molecules which tends to reduce when compared with the bulk phase prop-erties. Several experimental and theoretical reports have been devoted to understand the unusual dynamics of water under con-finement [26–32]. Orientation and diffusion mechanisms of water molecules in the vicinity of a surface is still unclear. These reports reveal that polarity, hydrogen bonding (H-bonding) and orientation play a vital role for diffusion of water molecules.

Using a molecular dynamics (MD) approach, we were recently able to tackle the question of the interstitial bone fluid flows at the nanoscale [5]. These preliminary results have suggested that mobile water can be observed within HAP pores of the same size as the nanopores measured in bone by Holmes et al. [33]. Based on a molecular dynamics approach involving inter-atomic potentials models for HAP and water systems developed by Leeuw [34], this seminal study was well describing the HAP-water structure at the interface, but was badly adapted to properly describe the diffusive process of confined water [11]. That is why, in this paper, we intend to propose a comparison between different HAP-water models in

* Corresponding author.
E-mail address: thibault.lemaire@univ-paris-est.fr (T. Lemaire).

the perspective of their ability to describe properly the confined diffusion of water in nanopores.

The structure of this paper is therefore rather classical since the different water-HAP models are presented in a first Materials and methods section. In particular, the simulation strategy is presented. Then, a section is devoted to present the results and discuss their implications. The peculiar phenomenon of hydroxyl dissociation is also stressed out. Finally, conclusions and prospects are presented.

2. Materials and methods

2.1. Simulation boxes

HAP [Ca_{10} (PO_4)6 ($OH)_2$] is seen as a hexagonal primitive cell with $P6_3$ /m space group, each sphere representing a tetrahedral (PO_4^{3-}) ionic complex. Its natural organization in bone matrix corresponds to a stack of thin micro-plates with dimensions (L × l × e), where L = 250–500 Å, l = 150–250 Å and e = 25 Å [35]. That is why, similarly to the configuration in our previous study [11], the dimensions of parallelepipedic shaped simulation boxes are adjusted to contain (3 × 3 × 4) such micro-plates.

Due to partial occupancy of OH sites, the orientation of OH groups always protruded away from the surface (i.e. c axis). More-over, the simulation box contains a water layer whose height may be varied (in the c-axis direction) from 20 Å to 200 Å to mimic bone nanopores size. This variation of the water layer thickness is performed by adding or removing water molecules.

The position of each atom in the box is given using its Cartesian coordinates (x,y,z) in the orthogonal frame (e_1 ,e_2 ,e_3), see Fig. 1. The HAP platelets and water layers constitute the elementary cell which is repeated periodically along the $\mathbf{e}_3$ axis. The initial coordinates and crystal cell parameters were taken from [36].

2.2. Choice of different intermolecular interactions models

Four types of interatomic potential models were used to describe the interactions in the HAP nanopore-water systems. In the first model hereafter named CS-water, the interactions between particles were represented by the core shell interatomic potential developed by de Leeuw and Parker for HAP and water systems [18,37], which includes electronic polarizability via the shell model of Dick and Overhauser. This model was used in our previous studies [11,12]. In this CS-water model the phosphate, hydroxyl group, and oxygen–hydrogen (H_W) bonds are described as the sum of a Morse and a Coulombic potential, the phosphate and water bond angles by a harmonic potential, and non-bonded interactions by Buckingham potentials. This force field makes use of a shell model to represent the oxygen's electronic polarizability in the phosphate and hydroxyl groups, and in the water molecules, in which each oxygen atom consists of both a core and a massless shell connected by a spring.

In the second model, hereafter named LJ-SPC, the HAP interac-tions were described through Lennard-Jones potentials as proposed in [38] while water molecules were described by the SPC model.

The third model (noted LJ-SPC/E) is the same as the LJ-SPC except that the SPC/E water model was used instead. This is motivated by the good ability of the simple point charge (SPC/E) model to represent density, radial distribution functions, self-diffusion coef-ficient for water; and hydrogen-bond dynamics in good agreement with experiment [39–41]. The parameters set for the SPC and SPC/E models can be found in [39,40].

In the fourth model (noted CS-SPC/E) the core-shell representa-tion of the HAP mineral of de Leeuw and Parker [37] was combined with the SPC/E water model. This combination of potentials models was validated by activation energy (Ea) calculations [42].

The parameters of these models are listed in Table 1 and Sup-plementary Material (Tables S1 and S2).

2.3. Simulation process

Simulations were performed using the DL POLY molecular dynamics package (version 4.05.1) [43]. Each system was equili-brated in the microcanonical (NVE) ensemble for 50 ps, followed by 100 ps simulations in the isothermal–isobaric (NPT) ensemble, dur-ing which the volume was monitored in order to confirm the system reached equilibrium. The Melchionna modification of the Nosé-

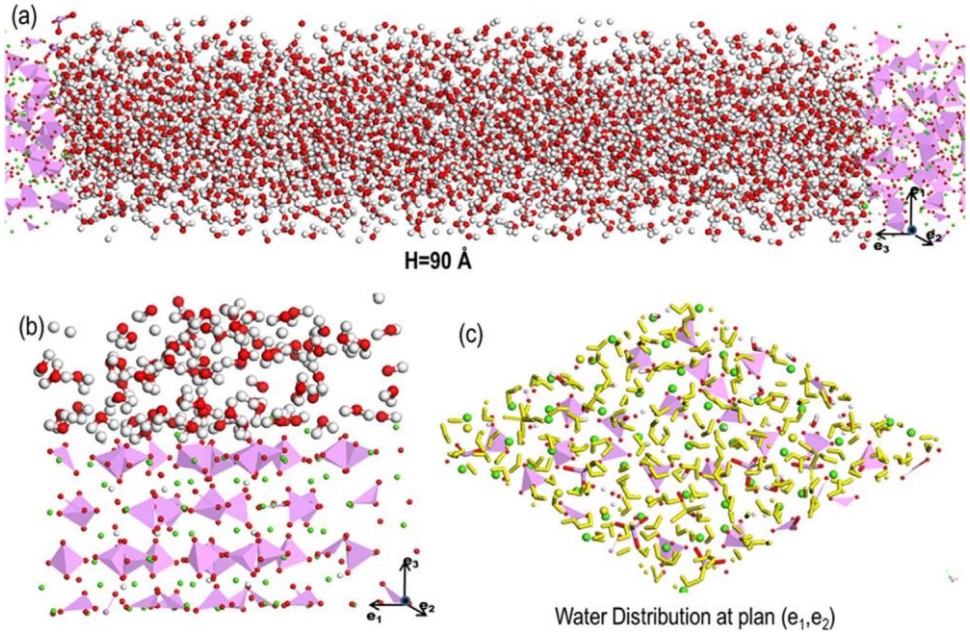

Fig. 1. Water-HAP system (Ca-green, PO_4^{3-} -pink, O-red, H-white): (a) Molecular arrangement of water molecules in a 90 Å HAP pore; (b) Interaction of water layers with surfaces; (c) Water layer (yellow) adsorbed on the HAP surface. (For interpretation of the references to colour in this figure legend, the reader is referred to the web version of this article.)

Table 1
Potential parameters used in this work for the Lennard-Jones and water models.

Atomic Partial Charges: (for LJ)			
Atom Types	Charges (e)		
Ca	+1.5		
P	+1.0		
Phosphate Oxygen (O2)	−0.8		
Hydroxy Oxygen (O1)	−1.1		
Hydroxy Hydrogen (H1)	+0.2		
Water Oxygen (Ow)	SPC = −0.82; SPC/E = −0.8476		
Water Hydrogen (Hw)	SPC = +0.41; SPC/E = +0.4238		
Lennard-Jones (LJ) Potential: $U(r) = 4\varepsilon_r \left(\frac{12}{-r}\right)^{6}$			
Ion Pair		(in kcal/mol)	(in Å)
Ca-O1		0.10198	3.5
Ca-O2		0.09539	3.35
O1-O1		0.08	3.7
O1-O2		0.07483	3.55
O2-O2		0.07	3.4
O_w—O1		0.1115	3.433
O_w—O2		0.104298	3.283
O_w—Ca		0.142434	3.233
O_w—O_w		0.1554	3.166
Harmonic Potential: $U(r) = \frac{1}{2} k(r - r_0)^2$			
Ion Pair		k(kcal/(mol.Å^2))	r_0 (Å)
P-O2		430	1.57
H1-O1		500	0.94
O_w -H_w		1108.2698	1.00
Three-body Potential: $U(\ ) = \frac{1}{2} k^{2} - 0$			
Ion Group		k(kcal/(mol.rad^2))	$_0$ (°)
O2-P-O2		125	109.47
H_w—O_w—H_w		91.5392	109.47

Hoover algorithm [44] was used with 0.5 ps for the thermostat and barostat relaxation times to maintain an average pressure of 1 atm and an average temperature of 310 K. This choice was made for comparison purpose with our previous work [11], which dealt with human bone environment under in vivo conditions. Thus, pores sizes typically range to classical bone nanopore sizes measured by [33] (between 50 Å and 125 Å).

Production runs in the NPT ensemble were then conducted for at least 2000 ps (i.e. 2 ns). The leap-frog algorithm with a time step of 0.1 fs was used to integrate the equations of motion. Periodic boundary conditions were applied in all directions of the box. The long range electrostatic interactions between the charges of all species were computed using the Smoothed Particle Mesh Ewald (SPME) method with the acceptable relative error of 10^{-6} [45]. The cut-off for calculation of the non-bonding interactions was set to 9 Å.

3. Results and discussion

3.1. Self-Diffusion coefficient of water

Our analysis is here focused on describing water diffusion pro-cess by depicting the self-diffusion coefficients of water for the different water models for various degrees of confinement, that is to say for various pore sizes.

The self-diffusion coefficients of water molecules D were calcu-lated from the mean-square displacement (MSD) using Einstein's expression:

$$D = \frac{1}{2} \frac{d}{dt} \left\langle [r(t) - r(0)]^2 \right\rangle \quad (1)$$

Here, r(t) corresponds to the position of a particle (water molecule) at time t. The chevrons notation stands for the averaging procedure.

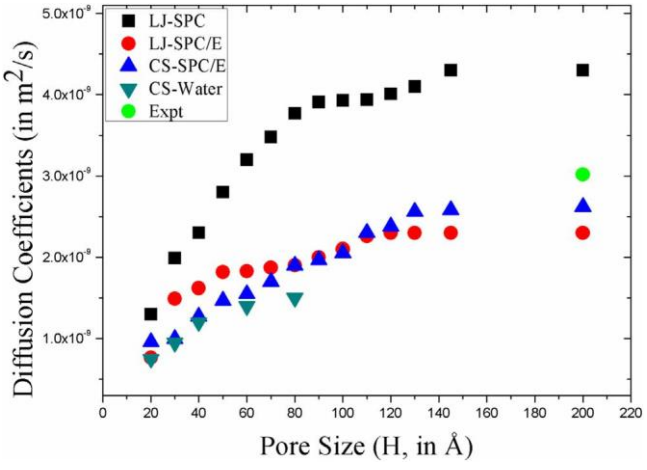

Fig. 2. Self-diffusion coefficients of water molecules calculated at 310 K for various pore sizes (H = 20 to 200 Å) with different potentials models: LJ-SPC, LJ-SPC/E, CS-SPC/E, CS-water. The experimental diffusion coefficient is also presented.

Fig. 2 displays the dependence of the self-diffusion coefficient D in terms of pore size H at 310 K for the four HAP-water inter-action potentials models. Note that the experimental bulk water self-diffusivity is also presented by the green bullet.

As expected, it is found from our calculation that the self-diffusivity of water gradually increases with the pore sizes, whatever be the type of interaction potential model.

Indeed, at 298 K for instance, the bulk water diffusion coef-ficients for SPC or SPC/E models are 3.85 and 2.3 × 10^{-9} m^2 s^{-1}, respectively [46]. Here, due to the confinement effect, the calcu-lated values are always lower even if the higher temperature should induce an increase in the water molecules mobility. This is due to

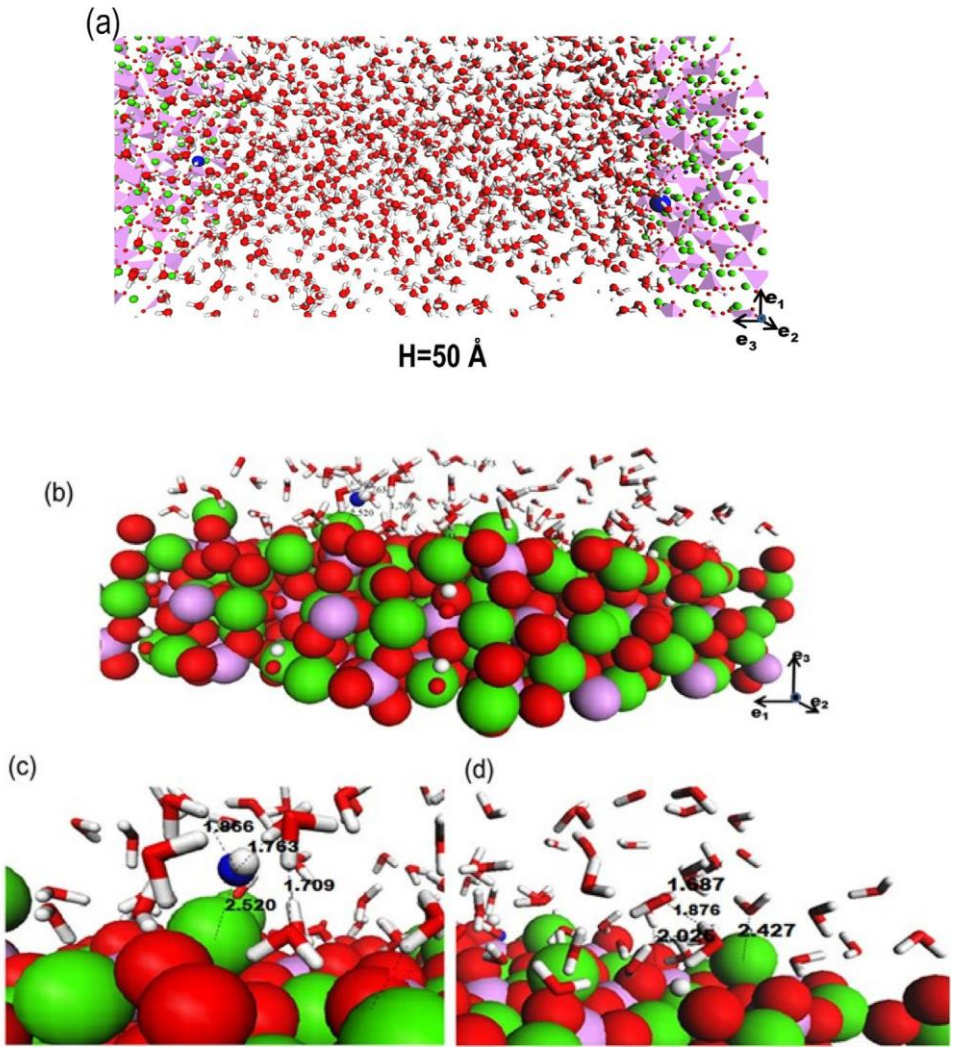

Fig. 3. Hydroxyl ions in HAP-Water system (Ca-green, PO_4^{3-} -pink, O-red, H-white and hydroxyl O-blue): (a) Molecular arrangement of water molecules and OH^- ions in a 50 Å HAP nanopore; (b) Interaction of OH^- ions with HAP-water layers; (c) and (d) shows the close views of H-bonds (distances are in Å) for OH^- -water and water-water, respectively, at the vicinity of HAP interface. (For interpretation of the references to colour in this figure legend, the reader is referred to the web version of this article.)

the strong electrostatic interactions between the HAP surface and water which tend to limit the diffusion process. This will also affect the orientation of water and cooperative effect between surround-ing water molecules. A similar trend has also been observed for the other nanoporous materials such as SiO_2 , Fe_3O_4 , CNT, and proteins [46].

When focusing on the differences between the different poten-tials models, it is first to notice that the LJ-SPC model always provides a much higher value of the water diffusivity than the other potentials models (LJ-SPC/E, CS-SPC/E, CS-water) which give more similar values. This may be explained by the charges of the SPC water model that are lower than the ones of the SPC/E model for instance, causing a faster diffusive transport.

Furthermore, for the small pores (H < 80 Å), it appears that the CS-water model of our previous study [11] and the CS-SPC/E present diffusion values that are slightly lower than the LJ-SPC/E predic-tions. For larger pores, this trend becomes the opposite.

It is interesting to note that for small pore sizes (between 20 and 50 Å), the confinement effect on the diffusivity coefficient is linear, whereas for larger pores, this is no more the case. This clearly states that two different kind of diffusion mechanism are possible in struc-tures presenting a HAP-water interface. This may be an evolution from a quasi 1D diffusion process in the narrow pores to anisotropic diffusion of water molecules for lower confinement [12].

Moreover, for the largest simulated pore size value H = 200 Å, that is to say for the weakest degree of confinement, it appears that the value obtained from the CS-SPC/E combination poten-tials model is in very close agreement with the experimental bulk water property. Indeed, a comparison of CS-SPC/E and LJ-SPC/E potentials models gives meaningful insights on the selection of suitable force field for the study of water in contact with HAP sur-face. For a 200 Å pore size, the CS-SPC/E calculated value of the water self-diffusion, respectively its experimental bulk value, is 2.62×10^{-9} m^2 s^{-1} , respectively 3.02×10^{-9} m^2 s^{-1} . This confirms earlier reports that concluded that CS potentials are more suited for describing the HAP-water interface phenomena [2].

The role of interstitial fluid flow in bone activity is central through its contribution to the transmission of remodeling sig-nals [47,48]. In particular, nanoscopic flows occurring inside the collagen-apatite matrix of bone may modify the vicinity of the osteocytes [5] which are key actors of bone adaptation. As a result, water diffusion occurring in the vicinity of the HAP crystals is an avenue of research of great interest in bone physiology.

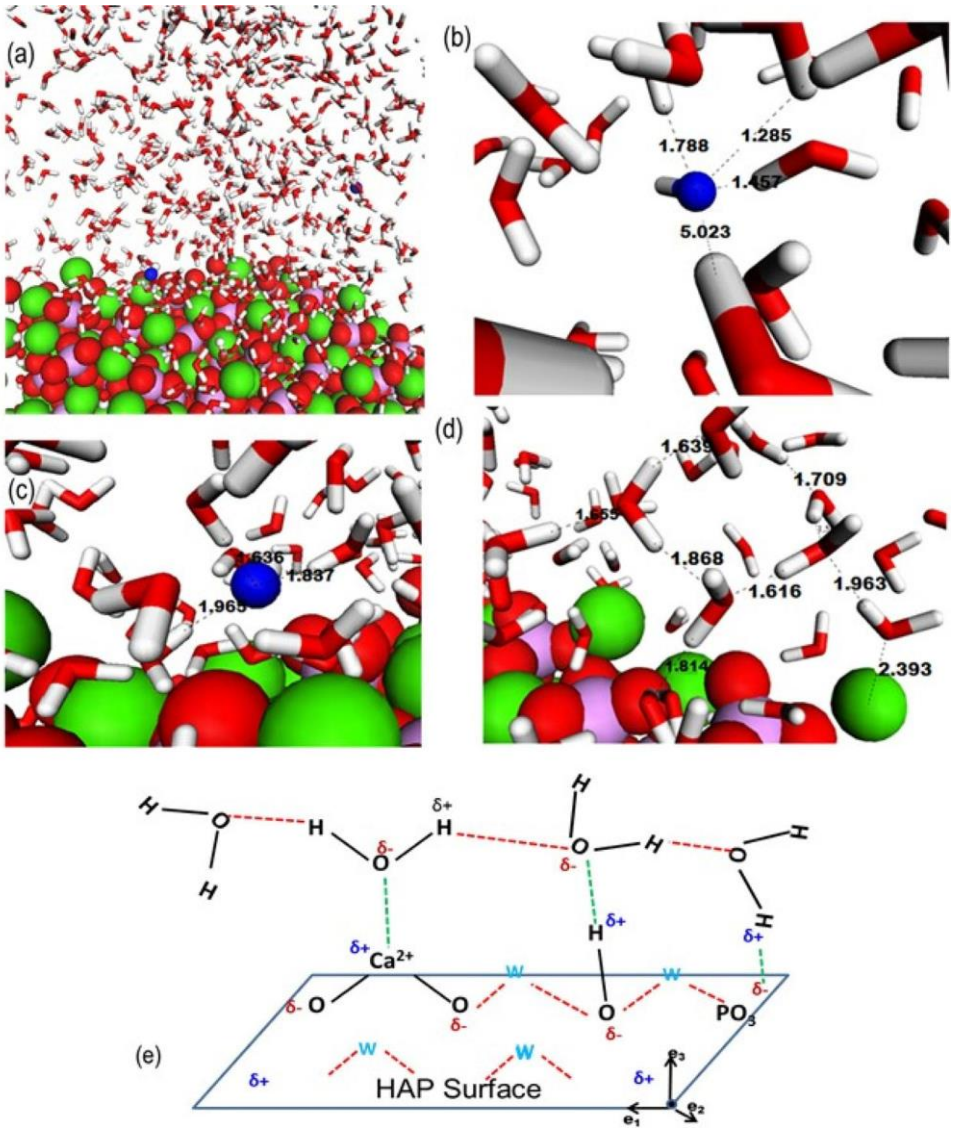

Fig. 4. Unusual hydroxyl ion diffusion in HAP-Water system (Ca-green, PO_4^{3-} -pink, O-red, H-white and hydroxyl O-blue): (a) Molecular arrangement of water molecules and OH^- ions in a 70 Å HAP pore; (b) and (c) Interactions of OH^- ion with water molecules near and far away from the HAP surface respectively; (d) H-bonded network between water molecules and Ca^{2+} -water interactions (Distances are in Å). (e) Schematic representation of HAP and water adsorption sites through H-bonding at interface. (For interpretation of the references to colour in this figure legend, the reader is referred to the web version of this article.)

3.2. Observation of hydroxyl ions dissolution

Due to the strong inductive effect from Ca ion and Ca-O_W bond, water molecules can adsorb/desorb at this interface. This phenomenon plays a role in the OH^- ion reorganization on HAP surface, and may locally affect the ionic concentration since we observed hydroxyl dissociation through our simulation with the CS-SPC/E model (see Figs. 3 and 4). This anionic specie tends to form multiple H-bonds (acting as a donor as well as acceptor) with the surrounding water molecules. Due to this effect, the transla-tional and rotational mobility of water molecules at this interface become unusual. To describe this phenomenon, atomistic modeling approach can give valuable information to understand the adsorp-tion/desorption and reorganization mechanism in HAP interface. This point is crucial during the biomineralization for instance.

It is interesting to note that from our calculations, the hydroxyl dissociation always depends on the pore size. In most of the cases, OH^- ions are dissociated and localized only near the surface (see Fig. 3) whereas in the case of medium pore sizes (i.e. H = 50–70 Å, see Fig. 4) we also observed OH^- ion slightly moving away from the HAP surface and becoming fully surrounded by water molecules via H-bonding interactions. Notice that H-bonding interactions between OH^- ion and water molecules are stronger and shorter compared to the normal water-water H-bonding interactions (see Fig. 4).

4. Conclusions and perspectives

We have conducted extensive molecular dynamics simulations of nanopores of HAP containing liquid water in order to deter-mine the effect of confinement on the diffusion properties of water by comparing various combination potentials models. When com-paring all these potentials models, it appears that the core-shell potential for HAP together with the SPC/E water model more accurately predicts the diffusion properties of water, the obtained values of the average diffusion coefficients being in good agree-ment with the experimental data from both bulk and bone-water interfaces [49–51].

Due to the strong interactions between water molecules and the functional groups of HAP which are dominant in such confined

environment, the diffusion in the nanopore direction is significantly faster than in the direction perpendicular to the HAP surface. As a result the diffusion process depends on H-bonding and orientation of water molecules on the surface. We showed that water molecules mainly interact with calcium ions, reducing its adsorption in the vicinity of the phosphate sites. Thus both Ca ion and OH groups protect the interaction between water and phosphate groups (Fig. S1).

Therefore we propose that strong inductive effect from Ca^{2+} and electrostatic interactions between water and surface tend to limit the diffusion process along the z-direction and at the same time induce the water molecules to move along x-direction via H-Bonded interactions. Our study can thus provide the valuable information to understand the mechanism of water movement dur-ing the biomineralization process.

Acknowledgements

The authors are grateful to Université Paris-Est Créteil (UPEC) which supported the French-English consortium. Moreover Muthuramalingam Prakash thanks UPEC for the financial support for his post-doctoral research grant.

References

[1] Ketul C. Popat, et al., Influence of engineered titania nanotubular surfaces on bone cells, Biomaterials 28 (21) (2007) 3188–3197.
[2] N.H. de Leeuw, Computer simulations of structures and properties of the biomaterial hydroxyapatite, J. Mater. Chem. 20 (26) (2010) 5376–5389.
[3] T. Lemaire, et al., On the paradoxical determinations of the lacuno-canalicular permeability of bone, Biomech. Model. Mechanobiol. 11 (7) (2012) 933–946.
[4] V. Sansalone, et al., Interstitial fluid flow within bone canaliculi and electro-chemo-mechanical features of the canalicular milieu, Biomech. Model. Mechanobiol. 12 (3) (2013) 533–553.
[5] T. Lemaire, et al., Water in hydroxyapatite nanopores: possible implications for interstitial bone fluid flow, J. Biomech. 48 (12) (2015) 3066–3071.
[6] A. Slepko, A.A. Demkov, First principles study of hydroxyapatite surface, J. Chem. Phys. 139 (4) (2013) 044714.
[7] Y.J. Yoon, S.C. Cowin, The estimated elastic constants for a single bone osteonal lamella, Biomech. Model. Mechanobiol. 7 (1) (2008) 1–11.
[8] V. Sansalone, et al., Nanostructure and effective elastic properties of bone fibril, Bioinspir. Biomim. Nanobiomater. 1 (3) (2012) 154–165.
[9] C. Hellmich, D. Katti, Multiscale mechanics of biological, bioinspired, and biomedical materials, MRS Bull. 40 (04) (2015) 309–313.
[10] Y. Wang, et al., Water-mediated structuring of bone apatite, Nat. Mater. 12 (12) (2013) 1144–1153.
[11] T.T. Pham, et al., Properties of water confined in hydroxyapatite nanopores as derived from molecular dynamics simulations, Theor. Chem. Acc. 134 (5) (2015) 1–14.
[12] M. Prakash, et al., Anisotropic Diffusion of Water Molecules in Hydroxyapatite Nanopores, Phys. Chem. Miner. (2017), in press.
[13] F. Chiatti, et al., Water at hydroxyapatite surfaces: the effect of coverage and surface termination as investigated by all-electron B3LYP-D simulations, Theor. Chem. Acc. 135 (3) (2016) 1–15.
[14] C. Oddou, et al., Hydrodynamics in porous media with applications to tissue engineering, in: K. Vafai (Ed.), Porous Media: Applications in Biological Systems and Biotechnology, CRC Press, Boca Raton, 2011, pp. 75–119.
[15] K. Kandori, et al., Adsorption of myoglobin onto various synthetic hydroxyapatite particles, Phys. Chem. Chem. Phys. 2 (9) (2000) 2015–2020.
[16] A. Rimola, et al., Ab initio modelling of protein-biomaterial interactions: influence of amino acid polar side chains on adsorption at hydroxyapatite surfaces, Philos. Trans. R. Soc. A 370 (1963) (2012) 1478–1498.
[17] M. Corno, et al., Hydroxyapatite as a key biomaterial: quantum-mechanical simulation of its surfaces in interaction with biomolecules, Phys. Chem. Chem. Phys. 12 (2010) 6309–6329.
[18] N.H. de Leeuw, Resisting the onset of hydroxyapatite dissolution through the incorporation of fluoride, J. Phys. Chem. B 108 (6) (2004) 1809–1811.
[19] N. Almora-Barrios, et al., Density functional theory study of the binding of glycine, proline, and hydroxyproline to the hydroxyapatite (0001) and (0110) surfaces, Langmuir 25 (9) (2009) 5018–5025.
[20] Y. Sakhno, et al., Surface hydration and cationic sites of nanohydroxyapatites with amorphous or crystalline surfaces: a comparative study, J. Phys. Chem. C 114 (39) (2010) 16640–16648.
[21] V. Bolis, et al., Coordination chemistry of Ca sites at the surface of nanosized hydroxyapatite: interaction with H2O and CO, Philos. Trans. R. Soc. Lond. A: Math. Phys. Eng. Sci. 370 (1963) (2012) 1313–1336.
[22] F. Chiatti, et al., Revealing hydroxyapatite nanoparticle surface structure by CO adsorption: a combined B3LYP and infrared study, J. Phys. Chem. C 117 (48) (2013) 25526–25534.
[23] W. Zhao, et al., Surface energetics of the hydroxyapatite nanocrystal–water interface: a molecular dynamics study, Langmuir 30 (44) (2014) 13283–13292.
[24] S.E.R. Hernandez, et al., The effect of water on the binding of glycosaminoglycan saccharides to hydroxyapatite surfaces: a molecular dynamics study, Phys. Chem. Chem. Phys. 17 (34) (2015) 22377–22388.
[25] L.S. Parvaneh, et al., Molecular mechanism of crystal growth inhibition at the calcium oxalate/water interfaces, J. Phys. Chem. C 120 (8) (2016) 4410–4417.
[26] A.R. Bizzarri, S. Cannistraro, Molecular dynamics of water at the protein-solvent interface, J. Phys. Chem. B 106 (26) (2002) 6617–6633.
[27] H.-S. Tan, et al., Orientational dynamics of water confined on a nanometer length scale in reverse micelles, J. Chem. Phys. 122 (17) (2005) 174501.
[28] J. Su, H. Guo, Effect of nanotube-length on the transport properties of single-file water molecules: transition from bidirectional to unidirectional, J. Chem. Phys. 134 (24) (2011) 244513.
[29] T.X. Nguyen, S.K. Bhatia, Some anomalies in the self-diffusion of water in disordered carbons, J. Phys. Chem. C 116 (5) (2012) 3667–3676.
[30] J. Das, et al., Anomalous diffusion of water molecules in hydrated lipid bilayers, J. Chem. Phys. 139 (6) (2013) 065102.
[31] T. Lemaire, et al., Bone water at the nanoscale: a molecular dynamics study, Comput. Methods Biomech. Biomed. Eng. 18 (Suppl. 1) (2015) 1982–1983.
[32] P. Rani, P. Biswas, Diffusion of hydration water around intrinsically disordered proteins, J. Phys. Chem. B 119 (42) (2015) 13262–13270.
[33] J.M. Holmes, et al., Gas adsorption and surface structure of bone mineral, Biochemistry 3 (12) (1964) 2019–2024.
[34] N.H. de Leeuw, A computer modelling study of the uptake and segregation of fluoride ions at the hydrated hydroxyapatite (0001) surface: introducing a Ca 10 (PO 4) 6 (OH) 2 potential model, Phys. Chem. Chem. Phys. 6 (8) (2004) 1860–1866.
[35] S. Weiner, W. Traub, Organization of hydroxyapatite crystals within collagen fibrils, FEBS Lett. 206 (1986) 262–266.
[36] K. Sudarsanan, R.A. Young, Significant precision in crystal structural details. Holly springs hydroxyapatite, Acta Crystallogr. Sect. B 25 (1969) 1534–1543.
[37] N.H. de Leeuw, S.C. Parker, Molecular dynamics simulation of MgO surfaces in liquid water using a shell-model potential for water, Phys. Rev. B 58 (1998) 13901–13908.
[38] T.-J. Lin, Force Field Parameters and Atomistic Surface Models for Hydroxyapatite and Analysis of Biomolecular Adsorption at Aqueous Interfaces. Phd Thesis, The University of Akron, 2013.
[39] H.J.C. Berendsen, et al., Interaction Models for Water in Relation to Protein Hydration: Intermolecular Forces, Springer, Netherlands, 1981, pp. 331–342.
[40] H.J.C. Berendsen, et al., The missing term in effective pair potentials, J. Phys. Chem. 91 (24) (1987) 6269–6271.
[41] M.F. Kropman, H.J. Bakker, Femtosecond mid-infrared spectroscopy of aqueous solvation shells, J. Chem. Phys. 115 (2001) 8942–8948.
[42] D. Di Tommaso, et al., Molecular dynamics simulations of hydroxyapatite nanopores in contact with electrolyte solutions: the effect of nanoconfinement and solvated ions on the surface reactivity and the structural, dynamical and vibrational properties of water, Crystals (2017), in press.
[43] I.T. Todorov, et al., DL POLY 3 (new dimensions in molecular dynamics simulations via massive parallelism), J. Mater. Chem. 16 (2006) 1911–1918.
[44] S. Melchionna, et al., Hoover NPT dynamics for systems varying in shape and size, Mol. Phys. 78 (3) (1993) 533–544.
[45] U. Essmann, et al., A smooth particle mesh Ewald method, J. Chem. Phys. 103 (19) (1995) 8577–8593.
[46] D. van der Spoel, et al., A systematic study of water models for molecular simulation: derivation of water models optimized for use with a reaction field, J. Chem. Phys. 108 (24) (1998) 10220–10230.
[47] S.P. Fritton, S. Weinbaum, Fluid and solute transport in bone (flow-induced mechanotransduction), Ann. Rev. Fluid Mech. 41 (2009) 347–374.
[48] T. Lemaire, et al., What is the importance of multiphysical phenomena in bone remodelling signals expression? A multiscale perspective, J. Mech. Behav. Biomed. Mater. 4 (2011) 909–920.
[49] R. Mills, Self-diffusion in normal and heavy water in the range 1–45 deg, J. Phys. Chem. 77 (5) (1973) 685–688.
[50] H. Weingärtner, Self diffusion in liquid water. A reassessment, Zeitschrift für Physikalische Chemie 132 (2) (1982) 129–149.
[51] P. Mark, L. Nilsson, Structure and dynamics of the TIP3P SPC, and SPC/E water models at 298 K, J. Phys. Chem. A 105 (43) (2001) 9954–9960.